

Bonding Characteristics Mediated by Saddle-Shaped Porphyrin Deformation: A Theoretical Approach to the Control of Spin State of Iron(III) Porphyrins

Ru-Jen Cheng* and Ping-Yu Chen^[a]

Abstract: Five-coordinate iron(III) porphyrin complexes can exist in high-spin ($S=5/2$), intermediate-spin ($S=3/2$), and admixed intermediate-spin ($S=5/2, 3/2$) states. It has been found that weak-field axial ligands, a small core size of porphyrin macrocycle, and saddle-shaped deformation of porphyrin macrocycle induces the contribution of intermediate spin to the ground state. While the experimental ground state depends on the nature of axial ligands and porphyrin macrocycles, EHT and INDO calculations on a series of five-coordinate iron(III) porphyrin complexes in this study suggest a clear crystal-field

explanation of the factors that can contribute to the stability of the intermediate-spin state. Based on our calculations, all these factors can increase the energy separation between the $d_{x^2-y^2}$ and d_{z^2} orbitals and between the $d_{x^2-y^2}$ and d_{xy} orbitals and contribute to the relative stability of intermediate-spin state. Saddle-shaped deformation of porphyrin decreases the symmetry ($C_{4v} \rightarrow C_{2v}$) of the coordination sphere and increases

the probabilities of bonding interactions between metal and macrocycle. It is the number of bonding interactions of saddle-shaped metalloporphyrins that elevates the energy of $d_{x^2-y^2}$ orbital. On the other hand, for the same symmetry rationalization, $d_{x^2-y^2}$ and d_{z^2} orbitals are extensively hybridized and induce large electronic structure asymmetry to the saddle-shaped iron(III) porphyrin complexes. A novel concept of *symmetry switch* to control the spin transfer pathway that may be critical to the biological activities in nature is proposed.

Keywords: iron • porphyrinoids • semiempirical calculations • spin states • symmetry switch

Introduction

Hemoproteins serve many diverse biological functions through the nearly identical heme prosthetic group as a consequence of the subtle coordination and redox chemistry apparent for iron porphyrins. A variety of oxidation (+2, +3, and +4) and spin (high, intermediate, and low) states of iron porphyrins, which are critical intermediates in the catalytic cycles of biological systems, have been extensively characterized by chemical model systems.^[1] The chemical variation of model heme complexes represents a very successful method for the elucidation of structure–property–activity interrelationships. A knowledge of these interrelationships may help to sort out the essential parameters that govern the specific action of the hemoproteins in biological processes. A major objective in synthetic and structural studies of iron porphyrin complexes has been to achieve an understanding of the control of the spin state of iron. A number of mechanisms by which the spin states of hemoproteins might be fine tuned

have been suggested. A primary determinant of the spin state is the nature and number of the axial ligands. The nature of the porphyrin ligand can also play an important role.

Five-coordinate iron(III) porphyrin complexes can exist as high-spin ($S=5/2$), intermediate-spin ($S=3/2$), and admixed intermediate-spin ($S=5/2, 3/2$) states. An argument which arises from crystal field theory for a tetragonal system suggests that the choice between an $S=5/2$ and $S=3/2$ spin state is directly governed by the energy separation between $d_{x^2-y^2}$ and the nearly degenerate d_{xy} , d_{xz} , and d_{yz} orbitals. This implies that no relatively stable quartet state should be found without changing the basic iron–porphyrin coordination (that is, increasing the σ -donor or π -acceptor ability of porphyrin macrocycle). However, most of the intermediate-spin iron(III) porphyrin systems reported up to now were controlled by the axial ligand field strength (for example, ClO_4^- , CF_3SO_3^- , and $\text{C}(\text{CN})_3^-$ and so on).^[2–7] The concept of magnetochemical series has been developed by Reed et al. to rank the relative field strengths of ligands based on the characteristics of admixed spin states.^[8] Perturbation of the ligand field in the axial direction (z) may only affect the splitting of d orbitals in the equatorial (x, y) plane indirectly.

Systematic studies of the coordination chemistry of non-planar porphyrins from our laboratory have demonstrated that saddle-shaped ring deformations of the porphyrin macro-

[a] Prof. Dr. R.-J. Cheng, P.-Y. Chen
Department of Chemistry, National Chung-Hsing University
Taichung, Taiwan, 402 (Republic of China)
Fax: (+886) 4-286-2547
Email: rjcheng@mail.nchu.edu.tw

cycles should be a natural way to stabilize the intermediate-spin state of iron(III) porphyrins.^[9] While both [Fe(OEP)Cl] and [Fe(TPP)Cl] are typical high-spin complexes, just by twisting the conformation of the macrocycle without changing the axial ligand, [Fe(OETPP)Cl] and [Fe(OMTPP)Cl] show properties with mixed intermediate-spin state.^[10] Nearly pure intermediate-spin ($S=3/2$) iron(III) complexes have been reported for phthalocyanines^[11, 12] and tetraazaporphyrin.^[13] It is widely accepted that it is the smaller hole of the macrocycle that makes the systems unusual.

Quantum mechanically mixed intermediate-spin states ($S=5/2, 3/2$) have been proposed for certain cytochromes *c'* and also for horseradish peroxidase.^[14] However, the structural rationale that may contribute to this unusual spin state in related biological systems remains unidentified. It is our goal in this research to explore all possible mechanisms derived from previous model studies with appropriate theoretical rationale. Five-coordinate heme complexes with admixed intermediate-spin nature that are representative of i) weak field axial ligand (i.e., [Fe(TPP)ClO₄] vs. [Fe(TPP)Cl] and [Fe(OEP)ClO₄] vs. [Fe(OEP)Cl]), ii) small core size of porphyrin macrocycle (i.e., [Fe(OETAP)Cl] vs. [Fe(OEP)Cl]), and iii) saddle-shaped deformation of porphyrin macrocycle (i.e., [Fe(OETPP)Cl] and [Fe(OMTPP)Cl] vs. [Fe(TPP)Cl] and [Fe(OEP)Cl]) for which crystal geometries are available will be analyzed by semiempirical molecular orbital calculations in our study. Calculations of the relative energies of high- and intermediate-spin states should provide important information about the relationship between structure and spin, and the factors that stabilize a particular spin state.

The use of INDO-ROHF calculations has been remarkably successful in predicting the spin-state ordering of the low-lying multiplets of numerous iron(III) porphyrins whenever the ligand types and geometries are known.^[15] Due to electron

correlation and orbital relaxation problems involved in INDO type calculations, Koopmans' approximation may not be used to estimate relative energies of molecular orbitals between closed shell and open shell, and generally will not offer a clear explanation with respect to crystal-field theory of the factors that can contribute to the stability of the intermediate-spin state. However, comparison within half-filled d orbitals obtained from high-spin systems should be informative. Extended Hückel theory (EHT) calculations generally yield orbitals of correct symmetry, and orbital energies roughly corresponding to molecular ionization potentials. EHT is the only semiempirical model that yields metal d orbitals as frontier molecular orbitals in a systematic fashion and supports crystal field ideas.^[16] On the other hand, EHT is too rough to include electron correlation and therefore is insensitive to the spin state of the complexes. Relative energies of d orbitals obtained from these two different semiempirical models (INDO vs. EHT) will be evaluated to establish our novel approach.

Computational Methods

Semiempirical calculations were performed to characterize the electronic structure and relative energies of the sextet and quartet states of the model heme complexes. In these studies, an INDO-based restricted open-shell Hartree-Fock formalism (INDO-ROHF) from the Cerius²/ZINDO program package (Molecular Simulations) that includes parameterization for transition metals was used.^[16, 17] The SCF calculations were then followed by a single excitation configuration interactions (CI). These CI were generated by the use of a Rumer diagram technique at level 10; this included 10 orbitals down the HOMO and 10 orbitals up the LUMO and consisted of approximately 200 configurations. The electronic configurations of the Fe^{III} center were assigned as $d_{xy}^1 d_{yz}^1 d_{xz}^1 d_{z^2}^1 d_{x^2-y^2}^1$ ($S=5/2$) and $d_{xy}^2 d_{yz}^1 d_{xz}^1 d_{z^2}^1$ ($S=3/2$) in the initial SCF cycles; these assignments were based on arguments from crystal-field theory. The notation corresponds to the orientation of the porphyrin macrocycle being in the *xy* plane with the pyrrole nitrogens placed, as near as possible, on the *x* and *y* axes. EHT calculations were performed with the program CACAO^[18] with a weighted-modified Wolfsberg-Helmholz formula.^[19] The literature Slater atomic orbital parameters were used for iron,^[20] and the standard ones for the main-group elements. Molecular geometries were transferred from the crystal structures available through Cambridge Structural Database (CSD) with appropriate symmetrizations. All the peripheral substituents on the porphyrin ring were replaced by hydrogens with C–H bond lengths of 1.08 Å. The molecular orbitals and states were labeled with the D_{4h} symmetry labels appropriate for planar four-coordinate metalloporphyrin, as is becoming conventional in porphyrin chemistry. The crystal structure of [Fe(OEP)Cl] is missing from the literature. A single crystal of [Fe(OEP)Cl] suitable for X-ray analysis was obtained by us and detailed structural data will be reported elsewhere.

Results and Discussion

Ground-state electronic structure: Table 1 shows the calculated energy differences in kcal mol⁻¹ between the $S=5/2$ and $3/2$ spin states, with the energy of the corresponding $S=5/2$ state used as a reference for the symmetrized crystal geometries of all model ferric heme complexes studied. Increasing the symmetry (from C_1) of the crystal geometries always lowered the energy of the system. Therefore the reasonably highest symmetry is imposed on each porphyrin skeleton as indicated in the table. Corresponding structural and electromagnetic properties^[2, 6, 9, 13, 21–23] including Fe–N_p bond lengths,

Abstract in Chinese: 五配位三價鐵紫質可以高自旋 ($S=5/2$)、中自旋 ($S=3/2$)、和混合中自旋 ($S=5/2, 3/2$) 等狀態存在。已知軸向配位基減弱、紫質大環孔徑縮小、以及紫質大環呈馬鞍型變形等都會造成中自旋在基態中的貢獻。本文中我們以 EHT 和 INDO 等計算方法對一系列五配位三價鐵紫質進行詳細的研究，對於影響中自旋穩定性的各項因素從晶場理論的觀點提供合理的解釋。計算結果顯示所有造成中自旋相對穩定性的因素都會增加 $d_{x^2-y^2}$ 和 d_{z^2} 軌域以及 $d_{x^2-y^2}$ 和 d_{xy} 軌域間的能量差。紫質呈馬鞍型變形降低其配位環境之對稱性 ($C_{4v} \rightarrow C_{2v}$)，增加金屬與紫質間產生鍵結作用的數目，而使 $d_{x^2-y^2}$ 軌域能量提高。另一方面，同樣受到對稱降低的影響， $d_{x^2-y^2}$ 和 d_{z^2} 軌域間發生強烈的混成，因而引發馬鞍型三價鐵紫質錯合物電子環境之高度不對稱性。在此我們提出一個全新的概念，自然界中可能存在一種主導生物活性的“對稱開關”控制著未偶電子的傳遞路徑。

Table 1. Calculated relative energies, structural data, and magnetic properties of iron(III) porphyrin complexes.

	[Fe(TPP)Cl]	[Fe(OEP)Cl]	[Fe(OMTPP)Cl]	[Fe(OETPP)Cl]	[Fe(TPP)(ClO ₄)]	[Fe(OEP)(ClO ₄)]	[Fe(OETAP)Cl]
Fe–N _p [Å] ^[a]	2.070(9)	2.067(2)	2.034(6)	2.031(5)	2.001(5)	1.994(10)	1.929(7)
C _{4N} –N _p [Å] ^[b]	2.011	2.013	1.980	1.978	1.981	1.977	1.897
symmetry ^[c]	C _{4v}	C _{4v}	C _{2v}	C _{2v}	C ₁ (C _{4v}) ^[d]	C ₁ (C _{4v}) ^[d]	C _{4v}
ΔE(3/2 – 5/2) ^[e]	12.6	11.8	3.5	1.9	–3.8	–4.5	–9.5
Δ _O (INDO) ^[f]	3.98	4.01	5.09	5.28	5.04	5.10	5.10
Δ _O (EHT) ^[g]	2.49	2.50	2.65	2.60	3.20	3.23	3.36
Δ _T (INDO) ^[h]	0.85	0.82	2.67	2.94	2.92	2.91	2.54
Δ _T (EHT) ^[i]	1.26	1.28	1.41	1.36	2.13	2.24	2.46
μ _{eff} (μ _B)	5.9 (300 K)	≈ 5.9 (100 K)	4.7 ≈ 5.1 (300 K)	5.1 ≈ 5.2 (300 K)	5.2 (300 K)	4.8 (275 K)	3.92 (295 K)
g _⊥	6.0	6.0	5.3	5.2	4.75	4.37	3.98
g _∥	2.0	2.0	2.0	2.0	2.03	2.00	1.99
spin State	h.s.	h.s.	admixed i.s.	admixed i.s.	admixed i.s.	admixed i.s.	i.s.
S = 3/2	0%	0%	35%	40%	65%	82%	100%
S = 5/2	100%	100%	65%	60%	35%	18%	0%
ref.	[21, 22]	[23]	[9]	[9]	[2, 22]	[6, 22]	[13]

[a] N_p, porphinato nitrogen; [b] C_{4N}, center of the best plane of the four N_p. C₄–N_p, core size of porphyrin macrocycle; [c] Symmetry used for MO calculations; [d] Symmetry without the axial perchlorate; [e] ΔE(3/2 – 5/2), energy difference in kcal mol^{–1} between S = 3/2 and 5/2 spin states; [f] Δ_O(INDO), energy difference in eV between d_{x²–y²} and d_{xy} from INDO/SCF calculations; [g] Δ_O(EHT), energy difference in eV between d_{x²–y²} and d_{xy} from EHT calculation; [h] Δ_T(INDO), energy difference in eV between d_{x²–y²} and d_{z²} from INDO/SCF calculations; [i] Δ_T(EHT), energy difference in eV between d_{x²–y²} and d_{z²} from EHT calculations.

effective magnetic moments, ESR g values, and the estimated percentages of composite spin state are also given in Table 1.

Similar to previous results obtained by Axe and co-workers, the data in Table 1 show that the sextet state is indeed the ground state in the typical high-spin complexes [Fe(TPP)Cl] and [Fe(OEP)Cl], and it is definitively more stable than the quartet state by ≈ 12 kcal mol^{–1}. These results are consistent with all the structural and electromagnetic properties for these compounds, indicating a nearly pure high-spin ground state. For the formally intermediate-spin complex [Fe(OETAP)Cl], the quartet state is more stable than the sextet state by 9.5 kcal mol^{–1}. On the other hand, the calculated quartet states of [Fe(TPP)ClO₄] and [Fe(OEP)ClO₄] are only ≈ 4 kcal mol^{–1} more stable than their respective sextet states, and correspond to a dominant quartet ground state with significant quantum mixing from a sextet state. By contrast, the calculated sextet states of [Fe(OETPP)Cl] and [Fe(OMTPP)Cl] are only 1.9 and 3.5 kcal mol^{–1} more stable than their respective quartet states, and correspond to a dominant sextet ground state with significant quantum mixing from a quartet state. Consistent with all the experimental data, relative stability of intermediate-spin state increases systematically from [Fe(TPP)Cl] toward [Fe(OETAP)Cl]. Figure 1 shows a nice linear correlation between ΔE(3/2 – 5/2) and Fe–N_p bond lengths. The Fe–N_p bond length is a fairly good indicator of the spin state if we confine the complexes to five-coordinate iron(III) porphyrins. These results again demonstrate the capability of semiempirical INDO-ROHF calculations to predict the ground state electronic structure of various iron(III) porphyrins including saddle-shaped porphyrins.

Crystal-field d-orbital splitting: Energies of the five d orbitals in the high-spin state obtained from INDO calculations for all iron(III) porphyrins studied are shown as correlation energy level diagrams in Scheme 1. Contributions of the d orbitals in each molecular orbital are represented as coefficients in front of the corresponding d orbitals. It is our expectation that in the

d⁵ high-spin state with all five d orbitals singly occupied, the relative energies of the d orbitals should offer the pattern of d-orbital splitting derived from crystal-field theory. To confirm the feasibility of this methodology, the corresponding results from EHT calculations shown in Scheme 2 can be used for qualitative comparison.

As can be seen from these two schemes, the energy separations between the d_{x²–y²} and d_{xy} orbitals (Δ_O) are significantly larger for the complexes with intermediate-spin contribution. However, it is worth mentioning that the correlation between Δ_O and Fe–N_p bond lengths is better for the data from EHT calculations than those from INDO calculations (Figure 2). Similar correlation between the energy separations of d_{x²–y²} and d_{z²} orbitals (Δ_T) and Fe–N_p bond lengths has also been recognized. The EHT theory is a ligand-field-based theory and the superiority of the results from EHT calculations will be rationalized through different type of bonding interactions between metal and porphyrin macrocycle in these two semiempirical models (vide infra).

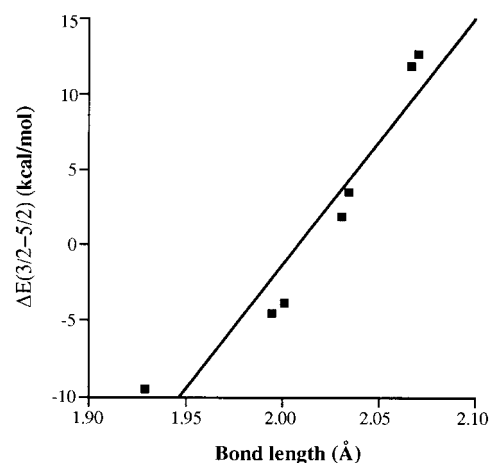
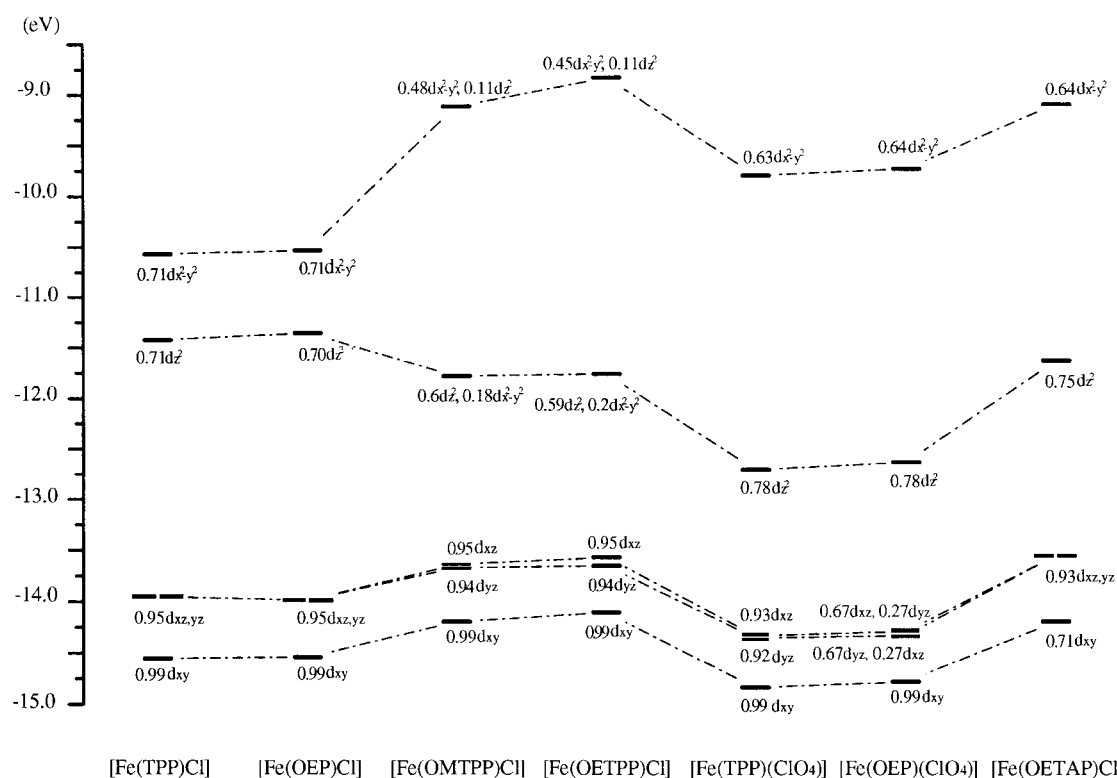
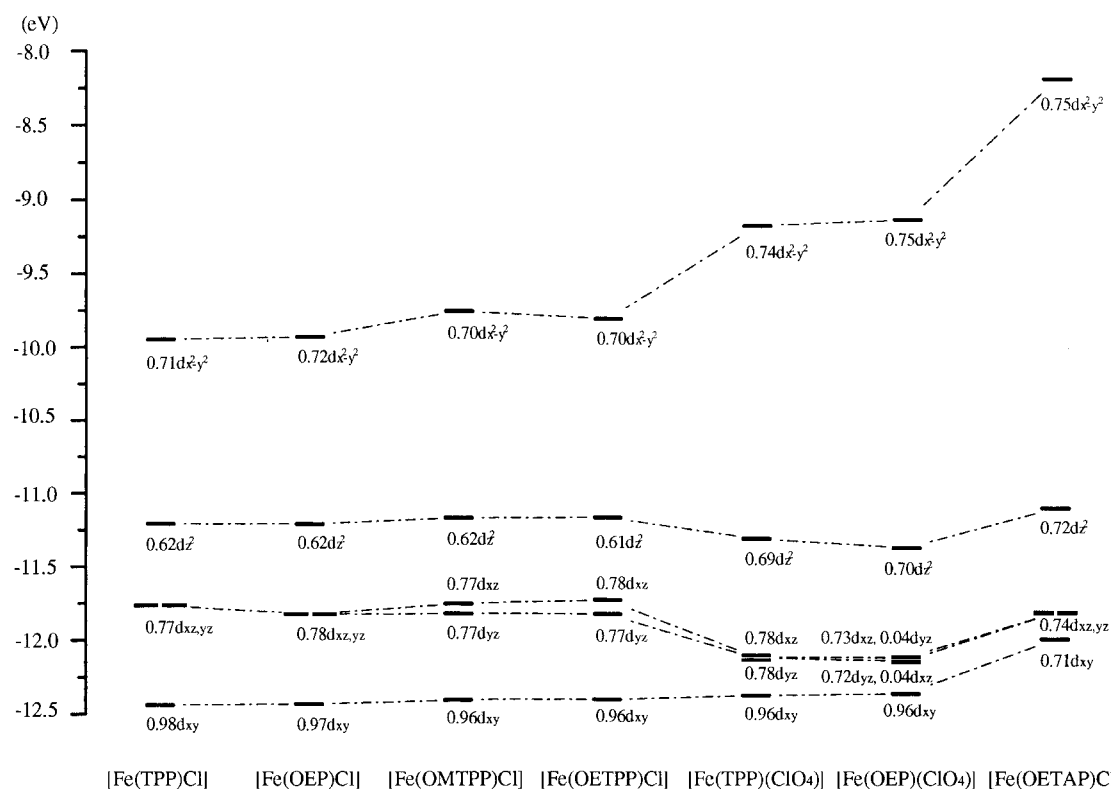


Figure 1. Energy differences between high- and intermediate-spin states calculated from INDO [ΔE(3/2 – 5/2)] vs. Fe–N_p bond lengths of iron(III) porphyrin complexes.



Scheme 1. Correlation energy-level diagram of the five d orbitals in the high-spin state obtained from INDO/SCF calculations for iron(II) porphyrin complexes. Coefficients represent the major contributions of d orbitals in the corresponding molecular orbital.



Scheme 2. Correlation energy level diagram of the five d orbitals obtained from EHT calculations for iron(III) porphyrin complexes. Coefficients represent the major contributions of d orbitals in the corresponding molecular orbital.

Table 2 summarizes the calculated closed-shell and open-shell electron populations of the iron d orbitals for both high-spin and intermediate-spin states of each complex. For the

high-spin states, the closed-shell populations represent the electron-density donation from either the axial ligand or the porphyrin, and the open-shell populations are related to the

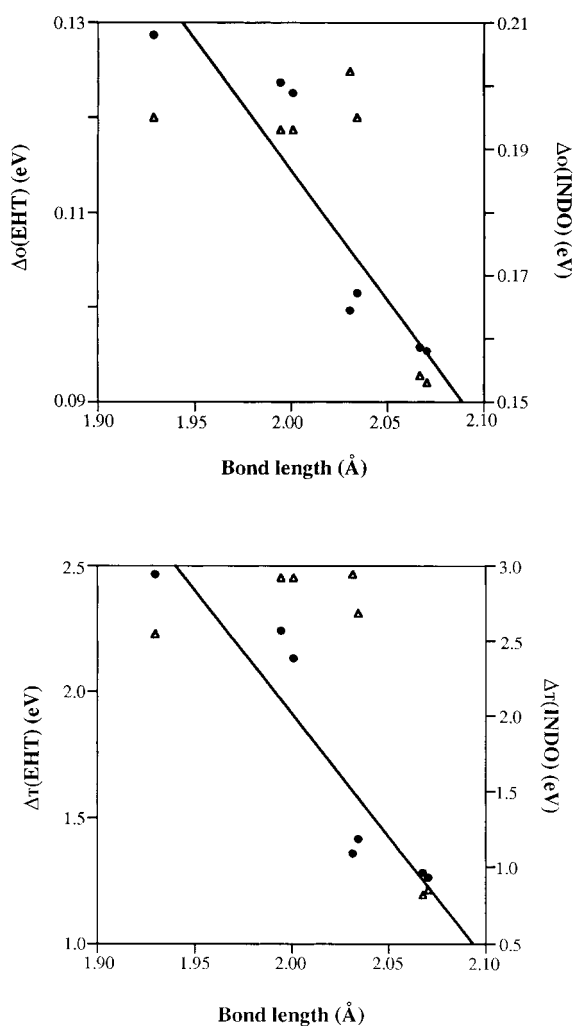


Figure 2. Energy differences between $d_{x^2-y^2}$ and d_{xy} orbitals (Δ_o) and between $d_{x^2-y^2}$ and d_{z^2} orbitals (Δ_π) from EHT (●) and INDO/SCF (△) calculations vs. Fe–N_p bond lengths of iron(III) porphyrin complexes.

unpaired spin density left over from bonding interactions. Generally, increasing closed-shell populations and decreasing open-shell populations indicate increasing bonding interactions between metal and ligands. Table 3 displays the calcu-

Table 3. Net charges and (unpaired spins) on Fe, the axial ligand, and porphyrin in the high- and intermediate-spin iron(III) porphyrin complexes from INDO calculations at SCF level.

	Fe	Ligand	Porphyrin
high-spin states			
[Fe(TPP)Cl]	1.33(4.32)	−0.75(0.14)	−0.58(0.54)
[Fe(OEP)Cl]	1.32(4.31)	−0.74(0.13)	−0.58(0.56)
[Fe(OMTPP)Cl]	1.35(4.26)	−0.76(0.13)	−0.59(0.61)
[Fe(OETPP)Cl]	1.36(4.24)	−0.77(0.13)	−0.59(0.63)
[Fe(TPP)(ClO ₄)]	1.31(4.30)	−0.74(0.06)	−0.57(0.64)
[Fe(OEP)(ClO ₄)]	1.31(4.30)	−0.74(0.06)	−0.57(0.64)
[Fe(OETAP)Cl]	1.50(4.23)	−0.76(0.14)	−0.74(0.63)
intermediate-spin states			
[Fe(TPP)Cl]	1.23(2.69)	−0.78(0.12)	−0.45(0.19)
[Fe(OEP)Cl]	1.22(2.70)	−0.77(0.12)	−0.45(0.18)
[Fe(OMTPP)Cl]	1.23(2.73)	−0.79(0.09)	−0.44(0.18)
[Fe(OETPP)Cl]	1.23(2.74)	−0.80(0.09)	−0.43(0.17)
[Fe(TPP)(ClO ₄)]	1.19(2.75)	−0.76(0.05)	−0.43(0.20)
[Fe(OEP)(ClO ₄)]	1.19(2.75)	−0.76(0.05)	−0.43(0.20)
[Fe(OETAP)Cl]	1.38(2.66)	−0.80(0.12)	−0.58(0.22)

lated Mulliken net charges and unpaired spin densities for the iron atom, the axial ligand, and the porphyrin ring for each complex.

Table 2 shows that in the high-spin complexes the d_{xy} , d_{xz} , and d_{yz} orbitals, with open-shell populations near one and closed-shell populations near zero, contribute very little to the spin delocalization and have no significant electron density from ligand-to-metal donations. These results indicate that d_{xy} is almost a nonbonding orbital, and π -bonding interactions between d_{xz} and d_{yz} orbitals and porphyrin macrocycles are negligible. By contrast, the $d_{x^2-y^2}$ orbital contributes significantly to the spin delocalization on the porphyrin ring. As shown in Table 3, the total unpaired electron density on the porphyrin ring is about 0.5 electrons for these compounds. Similarly, the d_{z^2} orbital contributes mainly to the spin delocalization on the axial ligand. Both $d_{x^2-y^2}$ and d_{z^2} orbitals are also recipients of substantial forward donation of electron density from both the axial ligand and the porphyrin ring, as shown by the significant closed-shell populations of these two orbitals and the reduced net formal charge on the ferric ion. All these interpretations are consistent with the patterns of d-orbital splitting shown in Schemes 1 and 2, in which the d_{xy} ,

Table 2. Mulliken closed-shell (open-shell) populations from INDO calculations at SCF level for the iron d orbitals in the high- and intermediate-spin iron(III) porphyrin complexes.

	$d_{x^2-y^2}$	d_{z^2}	d_{xz}	d_{yz}	d_{xy}
high-spin states					
[Fe(TPP)Cl]	0.554(0.718)	0.556(0.712)	0.100(0.947)	0.100(0.947)	0.015(0.992)
[Fe(OEP)Cl]	0.556(0.717)	0.575(0.702)	0.092(0.951)	0.092(0.951)	0.015(0.991)
[Fe(OMTPP)Cl]	0.660(0.663)	0.550(0.714)	0.094(0.951)	0.109(0.941)	0.020(0.989)
[Fe(OETPP)Cl]	0.685(0.650)	0.565(0.706)	0.091(0.953)	0.102(0.944)	0.021(0.988)
[Fe(TPP)(ClO ₄)]	0.701(0.643)	0.374(0.796)	0.119(0.937)	0.115(0.940)	0.024(0.987)
[Fe(OEP)(ClO ₄)]	0.701(0.643)	0.385(0.790)	0.117(0.938)	0.114(0.941)	0.025(0.986)
[Fe(OETAP)Cl]	0.681(0.649)	0.474(0.746)	0.140(0.926)	0.140(0.926)	0.035(0.980)
intermediate-spin states					
[Fe(TPP)Cl]	0.579(0.000)	0.406(0.783)	0.087(0.953)	0.087(0.953)	1.997(0.000)
[Fe(OEP)Cl]	0.583(0.000)	0.406(0.783)	0.081(0.956)	0.081(0.956)	1.997(0.000)
[Fe(OMTPP)Cl]	0.637(0.068)	0.411(0.753)	0.077(0.960)	0.085(0.950)	1.997(0.000)
[Fe(OETPP)Cl]	0.648(0.082)	0.421(0.743)	0.074(0.961)	0.079(0.953)	1.996(0.000)
[Fe(TPP)(ClO ₄)]	0.681(0.001)	0.264(0.843)	0.089(0.951)	0.089(0.953)	1.996(0.000)
[Fe(OEP)(ClO ₄)]	0.684(0.000)	0.267(0.842)	0.088(0.951)	0.086(0.954)	1.995(0.000)
[Fe(OETAP)Cl]	0.662(0.000)	0.381(0.785)	0.112(0.938)	0.112(0.938)	1.993(0.000)

d_{xz} , and d_{yz} orbitals are low lying and close in energy, while $d_{x^2-y^2}$ and d_{z^2} orbitals are obviously destabilized by antibonding interactions.

As shown in Tables 1 and 2, the complexes known to be with intermediate-spin contributions exhibit a significantly higher electron donation (increased closed-shell population) and spin delocalization (decreased open-shell population) between the $d_{x^2-y^2}$ and porphyrin ring, and a lower d_{z^2} orbital interaction with the axial ligand than in the formally high-spin complexes. The net effect of the increase in the $d_{x^2-y^2}$ interaction with the porphyrin and the decrease in the d_{z^2} interaction with the axial ligand is an increase in the energy separations between the $d_{x^2-y^2}$ and the d_{z^2} orbitals, and between the $d_{x^2-y^2}$ and the d_{xy} orbitals (Schemes 1 and 2); this results in the enhanced stability of intermediate-spin state.

Bonding interactions between metal and axial ligands: The axial ligands are the primary determinants of spin state.^[1] It is generally accepted that one of the conditions for favoring an intermediate spin in a complex is weaker axial ligand. However, it was frequently quoted that perturbation of the ligand field in the axial direction (z) should not affect the splitting of d orbitals in the equatorial (x, y) plane. Since the choice between an $S = 5/2$ and an $S = 3/2$ spin state is directly governed by the separation of the d_{xy} and $d_{x^2-y^2}$ orbitals, a rationale for how a change of the axial ligand field can affect the equatorial ligand field must be developed. An interesting compensating dependence of the equatorial ligand field of the porphyrin upon that of the axial ligand has been proposed by Reed et al.^[2] As the z axis ligand decreases its charge interaction with the iron atom a compensating increase in attraction of the equatorial ligands will occur. In crystal-field theory the center of gravity of the energy levels remains constant, therefore if the $d_{x^2-y^2}$ orbital goes up in orbital energy, others such as d_{z^2} might be expected to go down, and visa versa, even in the absence of other geometric changes. In addition, a stronger z -axis ligand might well pull the iron atom further out-of-plane and reduce the $d_{x^2-y^2}$ orbital energy as the d_{z^2} orbital energy goes up.

In agreement with Reed's compensating model, when the axial ligand field descends from chloride to perchlorate, there is a significantly lower electron donation (decreased closed-shell population) and spin delocalization (increased open-shell population) between the d_{z^2} orbital and the axial ligand and a concomitant higher $d_{x^2-y^2}$ orbital interaction with the porphyrin ring (Table 2). The net effect of the decrease in the d_{z^2} interaction with the axial ligand and the increase in the $d_{x^2-y^2}$ interaction with the porphyrin is an increase in the energy separations between the $d_{x^2-y^2}$ and the d_{z^2} orbitals and between the $d_{x^2-y^2}$ and the d_{xy} orbitals (Schemes 1 and 2); this results in the enhanced stability of intermediate-spin state. It is the change of these bonding interactions triggered by weakening of the axial ligand that makes $[\text{Fe}(\text{TPP})(\text{ClO}_4)]$ and $[\text{Fe}(\text{OEP})(\text{ClO}_4)]$ stable as mixed intermediate-spin complexes.

Bonding interactions between metal and porphyrin: For the six-coordinate iron(III) porphyrin (P) complexes, $[\text{Fe}(\text{P})\{3\text{-Cl}(\text{py})\}_2]\text{ClO}_4$, changes in the heme environment have been

shown to effect a change in spin state. Complexes with more basic porphyrinate ligands have higher spin multiplicity.^[24] However, in the case of five-coordinate complexes, $[\text{Fe}(\text{P})\text{Cl}]$, there is no evidence to show the control of spin state by porphyrin basicity. While $\text{p}K_3$ of OEPH_2 and TPPH_2 are about 4.36 and 3.95, respectively, both $[\text{Fe}(\text{OEP})\text{Cl}]$ and $[\text{Fe}(\text{TPP})\text{Cl}]$ are on the extreme of pure high-spin state. Our calculations, which are carried out for frozen crystal geometries, faithfully predict the spin states without porphyrin substituents. This indicates that the substituents have little electronic effect, at least in our model compounds, on the spin state of the complex. Actually, the electronic effect of the substituents has been merged into the changes of the coordination sphere. Bond lengths of $\text{Fe}-\text{N}_p$ did show significant difference between OEP and TPP complexes, and the calculated energy gaps between $d_{x^2-y^2}$ and the d_{z^2} orbitals also fall in the right direction. Following this trend, it should be possible to increase the contribution of intermediate-spin state of iron(III) by further increase the basicity of porphyrin macrocycle. Porphyrin basicity may be increased by strongly electron donating substituents that add directly to the porphyrin macrocycle, core size contraction of porphyrin macrocycle,^[13] or through saddle-shaped deformation of porphyrin macrocycle,^[25, 26] which seems to be less intuitively obvious. It is our expectation to obtain a direct mechanistic link between the structural feature and a change in iron spin state from molecular orbital calculations.

Tetraazaporphyrin (TAP) is composed of four pyrrole rings bridged by four aza nitrogen atoms. Owing to shorter bond distances between the pyrrolic α -carbon and the bridging nitrogen atoms and smaller bond angles about the bridging nitrogen atoms, the pyrrole rings of the tetraazaporphyrin tend to squeeze together to form a smaller core size. Apparently, the smaller core size of the tetraazaporphyrin increases the bonding interactions between the $d_{x^2-y^2}$ orbital and pyrrolic nitrogens. As shown in Schemes 1 and 2, elevation of the energy of $d_{x^2-y^2}$ orbital in the tetraazaporphyrin complex splits the iron d orbitals to a greater extent than does a porphyrin, resulting in an intermediate-spin complex. As a result of a compensating effect in the $[\text{Fe}(\text{OETAP})\text{Cl}]$ complex, it is not evident that the energy of d_{z^2} orbital does not descend as much as in the perchlorate complexes.

The question remains what kinds of bonding interactions cause the change in energies of the $d_{x^2-y^2}$ and the d_{z^2} orbitals for saddle-shaped porphyrin complexes. An interesting rationalization has been derived through detailed analyses of energy level diagrams of the fragment molecular orbital for this series of complexes. Saddle-shaped deformation of porphyrin decreases the symmetry ($C_{4v} \rightarrow C_{2v}$) of the coordination sphere and increases the probabilities of bonding interactions between metal and macrocycle. It is the number of bonding interactions of saddle-shaped metalloporphyrins that elevates the energy of $d_{x^2-y^2}$ orbital. On the other hand, for the same symmetry rationalization, $d_{x^2-y^2}$ and d_{z^2} orbitals are of the same symmetry (a_1) under the C_{2v} point group and can therefore be mixed. Extensive hybridization between $d_{x^2-y^2}$ and d_{z^2} orbitals will further increase the energy separation between them and make these two orbitals

distorted. As shown by the molecular orbital representations in Figure 3 and the coefficients in Scheme 1, it is impossible to find five conventional d orbitals that can be used for crystal-field rationalization in saddle-shaped porphyrin complexes. This may be the reason for the radical deviations of [Fe(OETPP)Cl] and [Fe(OMTPP)Cl] in Figure 2. Without this type of orbital mixing, results from EHT calculations (Figure 2) show much better d orbital energy difference correlations with Fe–N_p bond distances than that from INDO calculations.

It is very interesting to find that mixing of $d_{x^2-y^2}$ and d_{z^2} orbitals totally destroys the axial symmetry of the bonding interactions along *x* and *y* axes. While one hybridization shown in Figure 3a, composed mainly of $d_{x^2-y^2}$, has better

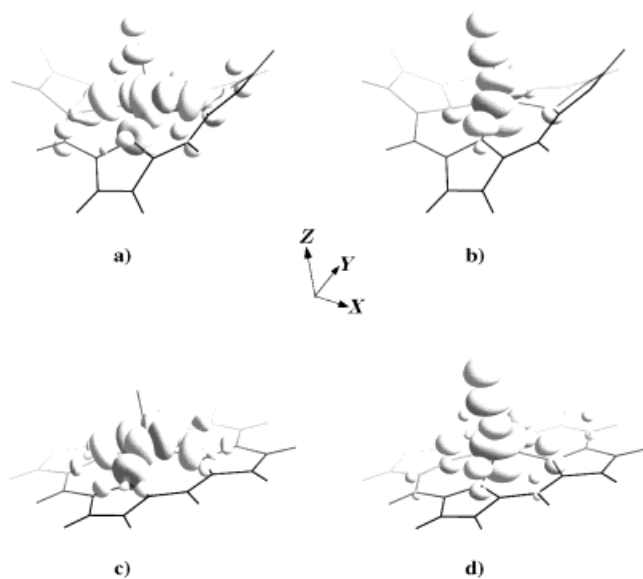


Figure 3. The hybridized molecular orbitals composed mainly of a) $d_{x^2-y^2}$ and b) d_{z^2} for [Fe(OETPP)Cl], and the molecular orbitals composed mainly of c) $d_{x^2-y^2}$ and d) d_{z^2} for [Fe(TPP)Cl].

bonding interactions along the *x* axis, the other hybridization shown in Figure 3b, composed mainly of d_{z^2} , is polarized along the *y* axis. This type of bonding anisotropy accompanied by the lowering of the spin multiplicity, which decreases the unpaired spin density in $d_{x^2-y^2}$ orbital, induces large electronic structure asymmetry in the saddle-shaped iron(III) porphyrin complexes.^[9] From this point of view, saddle-shaped ring deformation lowers the symmetry of the complexes, polarizes the pathway of spin transfer within porphyrin skeleton, and can be treated as a symmetry switch for spin transfer. Similar mechanisms of macrocycle distortions have been perceived to facilitate orbital mixing between a_{1u} and a_{2u} for porphyrin π -cation radicals and result in spin density redistribution.^[27] The potential generality of the concept of a symmetry switch may provide a readily accessible and heuristically useful tool for the elucidation of the biological relevance of these conformation-controlled electronic configurations of hemo-proteins.

Conclusion

Different levels of semiempirical molecular-orbital calculations including EHT and INDO have long been applied separately to the study of different aspects of coordination chemistry. In this report, we demonstrate that, working in combination, these two different models complement each other and offer clear explanation with respect to crystal-field theory of the factors that can control the spin state of metal complexes. While INDO calculations are excellent for the differentiation of electronic structures, EHT calculations are more than good enough for crystal-field rationalizations of coordination chemistry. As far as crystal-field rationalizations were concerned, EHT is too good to be true; that is, its result is straight forward and easy to apply, but its physical reality is poor—it does not infer the hybridization between $d_{x^2-y^2}$ and d_{z^2} orbitals. On the other hand, INDO is too true to be good; that is, it corresponds so closely to reality that its results deviate from the simple crystal field theory. It is worth mentioning that, our calculations strictly correspond to pure spin states with no spin-orbit coupling interaction. Therefore, they cannot represent exactly the properties of mixed intermediate-spin state of the complexes.

Manipulation of the crystal-field of a ferric porphyrin may be accomplished through a weak-field axial ligand, a small core size of porphyrin macrocycle, and saddle-shaped deformation of porphyrin macrocycle; this contributes to the stabilization of the unusual intermediate-spin states. Ring deformation has been proposed as a mechanism to mediate the electronic structure of cytochrome *c*'. It is instructive to understand the biological relevance of this mechanism by our model system studies. The novel concept of a symmetry switch for spin transfer may play an important role in the control of biological activity in nature. Further pursuit of this issue is underway in our laboratory.

Acknowledgments

We are greatly indebted to Professor R.-W. Yu (National Gau-Hsiung Normal University) and Dr. M.-D. Su (National Tsing-Hua University) for their valuable suggestions, and Mr. C.-C. Wu (National Chung-Hsing University) for technical support. This work was supported by the National Center for High-Performance Computing and the National Science Council of Republic of China, Grant No. NSC87-2113-M005-003.

- [1] W. R. Scheidt, C. A. Reed, *Chem. Rev.* **1981**, *81*, 543–555.
- [2] C. A. Reed, T. Mashiko, S. P. Bentley, M. E. Kastner, W. R. Scheidt, K. Spartalian, G. Lang, *J. Am. Chem. Soc.* **1979**, *101*, 2948–2958.
- [3] A. D. Boersma, H. M. Goff, *Inorg. Chem.* **1982**, *21*, 581–586.
- [4] H. Goff, E. Shimomura, *J. Am. Chem. Soc.* **1980**, *102*, 31–37.
- [5] H. Masuda, T. Taga, K. Osaki, H. Sugimoto, Z.-I. Yoshida, H. Ogoshi, *Inorg. Chem.* **1980**, *19*, 950–955.
- [6] D. H. Dolphin, J. R. Sams, T. B. Tsin, *Inorg. Chem.* **1977**, *16*, 711–713.
- [7] A. Gismelseed, E. L. Bominaar, E. Bill, A. X. Trautwein, H. Winkler, H. Nasri, P. Doppelt, D. Mandon, J. Fischer, R. Weiss, *Inorg. Chem.* **1990**, *29*, 2741–2749.
- [8] C. A. Reed, F. Guiset, *J. Am. Chem. Soc.* **1996**, *118*, 3281–3282.
- [9] R.-J. Cheng, P.-Y. Chen, P.-R. Gau, C.-C. Chen, S.-M. Peng, *J. Am. Chem. Soc.* **1997**, *119*, 2563–2569.

- [10] Abbreviations used in this paper: OEP = dianion of octaethylporphyrin; TPP = dianion of *meso*-tetraphenylporphyrin; OETPP = dianion of octaethyltetraphenylporphyrin; OMTTP = dianion of octamethyltetraphenylporphyrin; OETAP = dianion of octaethyltetrazaporphyrin.
- [11] B. Kennedy, G. Brain, K. Murray, *Inorg. Chim. Acta.* **1984**, *81*, L29–L31.
- [12] B. Kennedy, K. Murray, P. Zwack, H. Homborg, W. Kalz, *Inorg. Chem.* **1986**, *25*, 2539–2545.
- [13] J. P. Fitzgerald, B. S. Haggerty, A. L. Rheingold, L. May, *Inorg. Chem.* **1992**, *31*, 2006–2013.
- [14] M. M. Maltempo, *J. Chem. Phys.* **1974**, *61*, 2540–2547.
- [15] F. U. Axe, C. Flowers, G. H. Loew, A. Waleh, *J. Am. Chem. Soc.* **1989**, *111*, 7333–7339.
- [16] M. C. Zerner, in *Reviews in Computational Chemistry, Vol. 2* (Eds.: K. B. Lipkowitz, D. B. Boyd), VCH, New York, **1991**, pp. 313–365.
- [17] M. C. Zerner, in *Metal–Ligand Interactions* (Eds.: N. Russo, D. R. Salahub), Kluwer Academic, Netherlands, **1996**, pp. 493–531.
- [18] C. Mealli, D. M. Proserpio, *J. Chem. Edu.* **1990**, *67*, 399–402.
- [19] J. H. Ammeter, H.-B. Burgi, J. C. Thibeault, R. Hoffmann, *J. Am. Chem. Soc.* **1978**, *100*, 3686–3692.
- [20] R. H. Summerville, R. Hoffmann, *J. Am. Chem. Soc.* **1976**, *98*, 7240–7253.
- [21] W. R. Scheidt, M. G. Finnegan, *Acta Crystallogr.* **1989**, *C45*, 1214–1216.
- [22] S. Mitra, in *Iron Porphyrins, Vol. 2* (Eds.: A. B. P. Lever, H. B. Gray), Addison-Wesley, Reading, Massachusetts, **1983**, pp. 1–42.
- [23] V. R. Marathe, S. Mitra, *J. Chem. Phys.* **1983**, *78*, 915–920.
- [24] D. K. Geiger, W. R. Scheidt, *Inorg. Chem.* **1984**, *23*, 1970–1972.
- [25] K. M. Barkigia, M. Dolores Berber, J. Fajer, C. J. Medforth, M. W. Renner, K. M. Smith, *J. Am. Chem. Soc.* **1990**, *112*, 8851–8857.
- [26] R.-J. Cheng, Y.-R. Chen, C.-E. Chuang, *Heterocycles* **1992**, *34*, 1–4.
- [27] a) C.-Y. Lin, S. Hu, T. Rush III, T. G. Spiro, *J. Am. Chem. Soc.* **1996**, *118*, 9452–9453; b) S. A. Sabilia, S. Hu, C. Piffat, D. Melamed, T. G. Spiro, *Inorg. Chem.* **1997**, *36*, 1013–1019.

Received: September 10, 1998 [F1337]